Pergamon

Int. J. Heat Mass Transfer. Vol. 39, No. 11, pp. 2353–2362, 1996

0017-9310/96 $15.00+0.00

0017–9310(95)00249–9

Cooling of a superheated surface with a jet mist flow

YU. A. BUYEVICH† and V. N. MANKEVICH

Department of Mathematical Physics, Urals State University, 620083 Ekaterinburg, Russia

(*Received* 22 *August* 1994)

Abstract—The previously developed model of dynamic and thermal interaction of dilute mist flow with hot bodies is applied to study heat exchange in the circumstance when an axisymmetric two-phase jet falls normally onto a plate, the temperature of which exceeds the boiling temperature of the dispersed liquid. Depending on their approach velocity, impinging droplets either rebound, or come in direct contact with the plate and eventually evaporate, thus providing for an essential increase in the total heat removal. Such a crisis causes the occurrence of a temperature interval in which heat transfer from the plate decreases as the plate temperature grows. The very existence and properties of the mentioned anomalous region are explained in a good agreement with experimental findings. The results are also generalized to heat transfer involving polydisperse spray jets. Copyright © 1996 Elsevier Science Ltd.

1. INTRODUCTION

Spray cooling of hot surfaces is practised in quite a number of industrial processes because of some evident advantages over other possible methods of cooling. Evaporation of droplets impinging upon a superheated surface considerably adds to the overall heat removal, and this makes the discussed type of cooling much more efficient as compared with that caused by air flow under otherwise identical conditions. At the same time, dilute mist flow has an advantage of being cheap against similar liquid flow, by preventing an excessive waste of the liquid. Traditional design of air-water and other two-phase cooling devices is commonly based on the use of various arrangements of jet-like flows with different properties and contents of the dispersed liquid. Representative examples of experimental set-ups and engineering applications are to be found in refs. [1–8].

In spite of a great deal of experimental observations accumulated to the present date, the matter of proper organization of a spray cooling process at any specific condition is substantially impeded by the absence of a comprehensive theoretical model that would allow for making reliable predictions about working characteristics of the process. Only purely empirical correlations have been suggested until now, conditions and precise parametric regions of applicability of the correlations being by no means firmly established. Tentative theoretical concepts called to elucidate the underlying physics are usually of much too general a nature to serve the purpose, not to mention that sometimes they seem to be basically wrong. A certain exception is provided by the authors' papers [9, 10] in which a consistent approach to treat the problem has been put forward. It implies consideration of two different partial problems. The first one is that of dynamic and thermal interaction of a single droplet with a surface heated over the liquid boiling temperature. The second problem concerns disperse flow around a cooled body, with allowance for the inertial capture by the body surface of those suspended droplets whose approach velocity exceeds a certain critical value. Solution of the former problem enables one to find this value and, thereby, to formulate a boundary condition at the surface that is sorely needed to resolve the latter problem. After that, the whole amount of the droplets that are not rejected by, but come in touching contact with, the surface and next evaporate can be calculated for various areas of the surface.

The intended goal of the present paper is two-fold. First, we are going to set an example of application of the general method of refs. [9, 10] by way of considering a significant particular problem. Second, since the problem appears to be extremely important by its own right, we propose to investigate it in considerable detail. In the following, the method is used to study heat transfer when an axisymmetric spray jet falls normally onto an overheated plate. This problem is also believed to be helpful while forming an opinion about peculiarities of heat removal from surfaces of other forms under more sophisticated operating conditions.

The mist is presumed to be dilute enough in order to ignore the interaction between droplets near and on the plate. It amounts to dealing merely with such plates and other surfaces that remain almost dry in the course of cooling. The impinging droplets are either elastically thrown away or captured by a surface and completely vaporize within a sufficiently short time,

† Present address: NASA Ames Research Center, Moffett Field, CA 94035-1000, U.S.A.

NOMENCLATURE

a	droplet radius
d	nozzle diameter
f	droplet flow rate distribution density
h	height of nozzle above plate
L	latent heat of evaporation
r	radial coordinate
$r_{0.5}$	length scale of jet flow
Q, q	overall heat removal and its density
Stk	Stokes number
T	temperature
U	longitudinal jet velocity
W_n, w	normal component of droplet impact velocity and its dimensionless value
x, z	longitudinal coordinates.

Greek symbols

α	coefficient in equation (9)
β, σ	dispersion coefficients involved in equation (11)
γ	droplet concentration
Δ	length scale of surface roughness
δ	length scales introduced in (1) and defined in (3)
η, ξ	dimensionless coordinates
λ	vapor thermal conductivity
μ	gas dynamic velocity
ν	vapor kinematic viscosity
ρ	liquid density.

Superscripts

*	boundary between zones III and IV of jet flow
+	dimensionless quantities introduced when using scales d and U_d.

Subscripts

c	critical
d	nozzle edge
e	evaporation
m	maximal
o	plate
s	saturation
w	wall (plate).

before the next droplet hits the same part of the surface. The diluteness requirement permits one to also neglect a possible effect of an outward flow of the vapor, that is released as a result of the droplet evaporation, on the motion of other droplets approaching the plate. Some other assumptions characteristic of the study in refs. [9, 10], such as neglect of the temperature dependence of all thermophysical and dynamic properties of both liquid and its vapor, are employed as well. An assumption that is worthy of being specially pointed out is that the droplets in the vicinity of the plate are supposed to be under the saturation conditions. In particular, their temperature is taken to be equal to that of boiling.

It is expedient to note just off hand that determination of the local heat take-off, caused by droplet vaporization on a superheated surface, necessarily involves a rather tedious and unwieldy numerical calculation. For instance, this is true even for bodies of simple forms in a uniform mist flow [9, 10] since the inertial capture problem is too complicated to be solved by analytical means, even though the gas velocity field around a body may be well known and described by simple formulae. The situation with a jet flow near a plate happens to be still more intricate, since the mentioned field is no longer to be described with the aid of ordinary analytical functions, and can be found in no other way but numerically. Unfortunately enough, this makes the results on heat transfer to be obtained not so transparent from a physical point of view, as they undoubtedly ought to be.

2. DESCRIPTION OF TWO-PHASE JET FLOW

We start with determination of hydrodynamic properties of mist flow originated by a submerged two-phase axisymmetric jet that falls normally on a plate through a stagnant environmental gaseous plate. To do this, we are going to avail ourselves of some standard semi-empirical methods and results of the conventional theory of turbulent jet flow listed in refs. [11–14]. A sketch of the jet flowing out of a nozzle is presented in Fig. 1. Four distinguishable flow zones

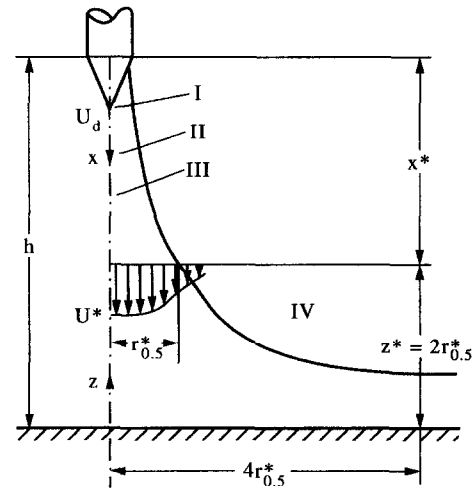

Fig. 1. A sketch of spray jet cooling; explanation in the text.

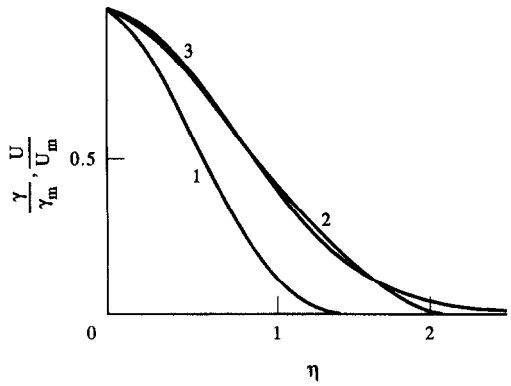

Fig. 2. Schlichting profiles of gas velocity (1) and droplet concentration (2) and Gaussian velocity profile (3).

may usually be singled out. Initial zone I is characterized by a unidirectional velocity profile depending on the nozzle type and a given regime of its performance. It is of no consequence for the goals of this paper. Intermediate zone II corresponds to gradual development of self-similar profiles of the longitudinal velocity components of the gas and droplets, that establish themselves in a boundary region between the intermediate zone and main zone III of the jet flow. The self-similar profiles throughout the latter zone are justly assumed to be approximately the same as for the corresponding free jet that is not affected by an obstacle downward the flow. These profiles may then be described with the aid of the semi-empirical model by Schlichting [11]. The flow becomes sensitive to the presence of the plate merely within a 'zone of plate influence' IV. A boundary dividing zones III and IV appears to be somewhat arbitrary in the same way as, in effect, are boundaries between all the other indicated zones. It can be reasonably defined on the basis of a hydrodynamic analysis of the gas and particle velocity fields.

The main zone is commonly believed to begin at distance $x = 5d$ from the nozzle, d being the nozzle diameter [11]. Profiles of the longitudinal gas velocity and droplet concentration within the last zone may be written down in a self-similar form [11].

$$U = (1-\eta_u^{3/2})^2 U_m \quad \eta_u = r/\delta_u$$
$$\gamma = (1-\eta_\gamma^{3/2})^2 \gamma_m, \quad \eta_\gamma = r/\delta_\gamma \qquad (1)$$

where δ_u and δ_γ are characteristic length scales related to each other as $\delta_u/\delta_\gamma = 1.5$ and U_m and γ_m are maximal values of U and γ reached at the jet symmetry axis $r = 0$ in any plane $x = \text{const}$. Profiles (1) are illustrated in Fig. 2. Obviously, U describes the local gas volume flux, whereas that of the dispersed liquid equals γU by definition if γ is understood as the fraction of the droplets by volume ($\gamma \ll 1$) and the longitudinal component of the droplet velocity coincides approximately with that of gas.

Dependence of both U and γ on longitudinal coordinate x is determined by those of U_m, γ_m and of δ_u, δ_γ. For free jets, there exist empirical formulae [12]

$$U_m = 8(3+0.85x/d)^{-1} U_d$$
$$\gamma_m = 8(3+0.85x/d)^{-1}\gamma_d \quad x/d > 6 \qquad (2)$$

with U_d and γ_d being understood as uniform values of the gas velocity and droplet concentration at the nozzle edge. Instead of either δ_u or δ_γ, it is natural to use the radial distance $r_{0.5}(x)$ from the jet axis at which the gas velocity equals half of its maximal value in a given plane $x = \text{const}$. There is an empirical law that determines this distance as a function of x in free submerged jets, also inside the main zone of the jet under study. Together with definitions of δ_u and δ_γ, this law can be written as follows [11]:

$$r_{0.5} = 0.09x, \quad \delta_u = 2.27 r_{0.5} = 0.20x,$$
$$\delta_\gamma = \delta_u/1.5 = 0.14x. \qquad (3)$$

These functions supplement those in equation (2) in the matter of elucidating the dependence on x of variables U and γ identified in equation (1).

Below we choose a plane $x = x^*$ ($z = z^*$), in which the deviation of actual function $U_m(x)$ from that in equation (2) amounts to about 1%, as a boundary between zones III and IV. Such a choice can be effected in practice only if the distance h separating the jet nozzle and the plate exceeds $6d$ [12], in which case formulae in equation (2) also hold approximately true. Then the thickness z^* of the zone of plate influence can safely be taken as $2r^*_{0.5} = 2r_{0.5}(x^*)$. Dependence of $r^*_{0.5}$ on h results from evident relations $h = x^* + 2r^*_{0.5}$ (see Fig. 1) and $r^*_{0.5} = 0.09x^*$ [see equation (3)], whence $r^*_{0.5} = 0.076h$ and $z^* = 0.152h$.

The gas velocity field **U(r)** within zone IV can be calculated numerically by following the procedure elaborated in refs. [13, 14]. Flows that are most commonly encountered in spray cooling processes are usually governed by pressure and inertia forces, and viscosity forces play only a minor role everywhere except a very thin boundary layer adjoining the surface of a cooled body. Furthermore, if the two-phase mixture under consideration is sufficiently dilute, the back influence of the droplets on gas flow may be overlooked. It is why the flow can be approximately described within the entire flow region as that of an ideal incompressible fluid. This permits the gas pressure and velocity fields to be found on a basis of standard equations for the flow stream function, which we are not going to write out here. Boundary conditions that must be imposed on the stream function and its space derivatives are pretty common as well [13, 14]. In particular, they include a condition of the longitudinal component of the gas velocity at $z = z^*$ being equal to quantity $U(x^*, r)$ that is identified in conformity with equations (1)–(3). The region of numerical integration of the equations may be determined by inequalities $0 < z < z^* = 0.152h$ and $0 \leqslant r < r^*$, with r^* to be chosen in such a manner as

to satisfy necessary requirements of accuracy of the calculation. Below we take $r^* = 4r^*_{0.5} = 0.304h$ which has been shown in ref. [13] to provide, as a rule, for sufficient accuracy.

The numerical calculation of **U(r)** founded on such a familiar formulation has been carried out in the same way as elsewhere (see examples in refs. [13, 14]), save for the replacing of the Schlichting velocity profile (1) by a Gaussian profile,

$$U = U_m \exp[-(\ln 2)\eta^2], \quad \eta = r/r_{0.5} \tag{4}$$

in order to simplify the calculation procedure. The mentioned profiles are compared between themselves in Fig. 2.

Results on the gas velocity field are needed solely to find out trajectories of droplets entering zone IV with the gas stream. The trajectories have to be determined by integrating the equation of motion of a single droplet which may be put forward in a dimensionless form [15]

$$Stk(d^2\zeta/d\tau^2) + d\zeta/d\tau = \boldsymbol{u}(\zeta) \quad \zeta = (\xi,\eta)$$
$$\{\xi,\eta\} = \{z,r\}/r^*_{0.5} \quad \tau = U^*t/r^*_{0.5}$$
$$Stk = 2\rho a^2 U^*/9\mu r^*_{0.5} \quad U^* = U_m(x^*) \tag{5}$$

where ρ is the liquid density, μ is the gas viscosity and a is the droplet radius. Quantities $r^*_{0.5}$ and U^* play the role of length and velocity scales, respectively. The 'initial' velocity of the droplets in plane $\xi = \xi^*$ ($z = a^*$) has been presumed to coincide with the longitudinal gas velocity, in accord with experimental evidence [11, 12].

Equation (5) forms a sound foundation to tackle manifold processes of inertial collection of fine particles by various bodies immersed into an aerosol flow. It is also extensively used while treating processes of particle deposition on walls of flow channels of different configuration. A general formulation of problems pertaining to the capture of droplets by a superheated surface [9, 10] remains basically the same as that of the inertial collection problems [15], save for using another condition of the droplets being actually retained by the surface.

3. CAPTURE OF DROPLETS BY THE PLATE

Equation (5), with its right-hand side evaluated numerically as explained above, serves to determine the field of droplet trajectories inside zone IV of plate influence. Each trajectory depends on the initial dimensionless radial coordinate $\eta = r/r^*_{0.5}$ of a droplet in plane $\xi = \xi^*$. Integration of equation (5) at the last condition and the condition of the droplet velocity being equal to that of gas at $\xi = \xi^*$ enables us to find dependence on η of the dimensionless radial coordinate $\eta_o = r_o/r^*_{0.5}$ at which the droplet will intersect plane $\zeta = 0$, as well as of the normal component $w = W_n/U^*$ of the dimensionless droplet velocity in this plane. These variables are plotted as functions of

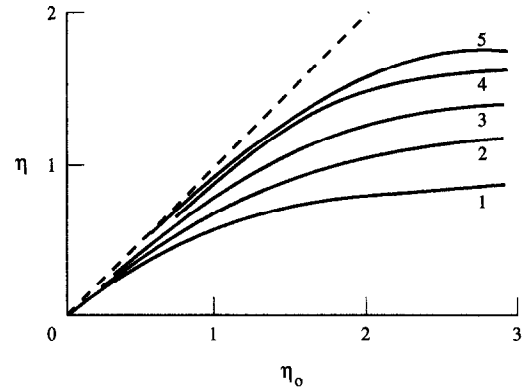

Fig. 3. Dependence of dimensionless radial coordinate η_o of droplet impact onto the plate on that in reference plane $z = z^*$ (η); 1–5—$Stk = 0.5$, 1, 2, 5, 10; dashed line corresponds to droplets which would approach the plate without dispersion.

η at different Stk on Figs. 3 and 4, respectively. Unlike flows around bodies of a finite size [15], it appears to be impossible to introduce an effective cross-section of inertial droplet collection by an unbounded plate, since there is no finite value of η corresponding to zero impact velocity W_n. It means that all the droplets would sediment on the plate, if their nearly elastic rebound were overlooked.

The curves of Fig. 3 serve to determine those points of the plate in which terminate the trajectories of the droplets of a given size that enter zone IV at different points η. They offer an opportunity to find the local flux of droplets coming to the plate. Really, the densities $f(\eta)$ and $f_o(\eta_o)$ of the droplet flow rate in planes $\xi = \xi^*$ and $\xi = 0$, respectively, are related to each other by an evident balance equation, $\eta f(\eta)\,d\eta = \eta_o f_o(\eta_o)\,d\eta_o$. Hence

$$f_o(\eta_o) = (\eta/\eta_o)(d\eta/d\eta_o) f(\eta) \tag{6}$$

with η being looked upon as a single-valued function of η_o, that corresponds to the curves of Fig. 3. These

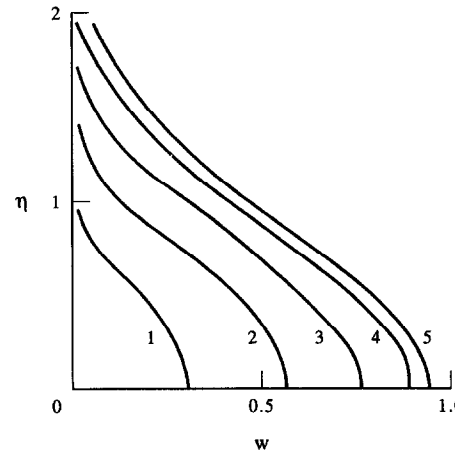

Fig. 4. Dependence of dimensionless droplet impact velocity on η; notation is the same as in Fig. 3.

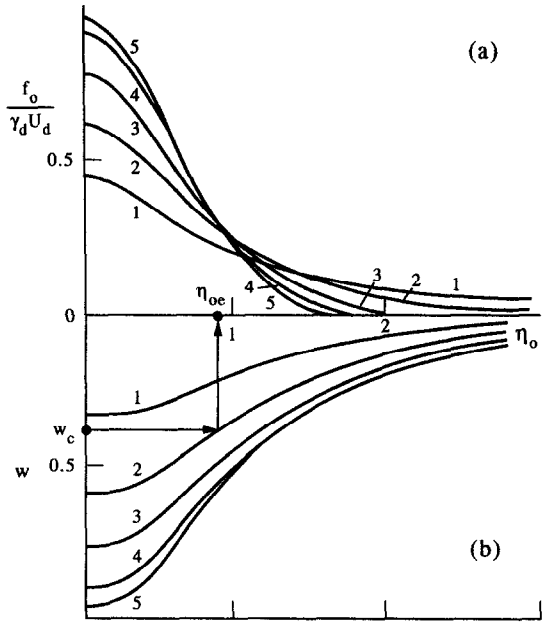

Fig. 5. Relative droplet flow density at the plate (a) and dimensionless impact velocity (b) as functions of η_o; notation is the same as in Fig. 3.

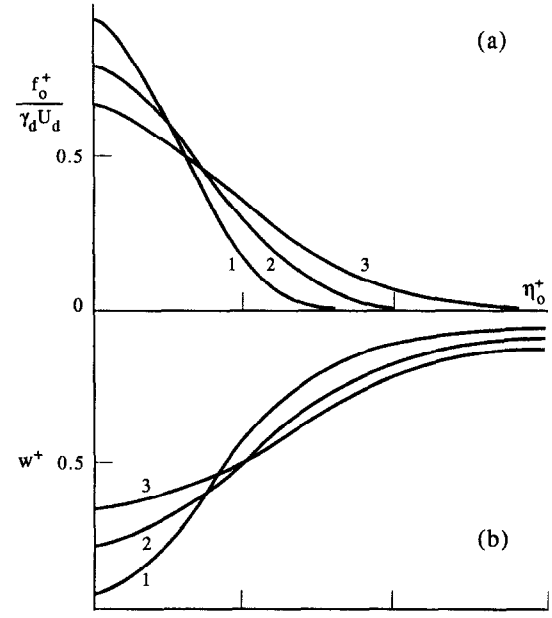

Fig. 6. Relative droplet flow density (a) and dimensionless impact velocity (b) as functions of η_o^+; $Stk = 10$; 1–3— $h/d = 6, 8, 10$.

flow rate densities may be normalized in an arbitrary way. If the volume flux of the dispersed liquid is under question, then $f(\eta)$ stands for γU in plane $x = x^*$, with arguments of γ and U in equation (1) being expressed through η with the help of equation (3).

When making use of equation (6) and of the curves in Figs. 2–4, it is not difficult to get dependencies on η_o of both f_o and w. The latter are demonstrated in Fig. 5 for droplets of different sizes (that is, at different Stk). When the droplets approach plane $\xi = 0$, the initial droplet flow rate density evolves in such a way as to become more and more gently sloping. This is all the more so, the smaller the droplet Stokes number.

Let W_c be a critical value of the droplet impact velocity, such that droplets with $W_n < W_c$ bounce off the plate due to the excessive pressure in thin vapor layers forming beneath the droplets as they approach the plane [9, 10], whereas those with $W_n > W_c$ come to direct contact with the plate and eventually vaporize. This value allows the dimensionless radius η_{oe} of a plate region where the evaporation takes place to be found for flow of identical droplets of any size. It is schematically shown with arrows on Fig. 5 for droplets with $Stk = 1$ at a certain $w_c = W_c/U^*$.

The usage of the same critical value of the droplet impact velocity in Fig. 4 gives an opportunity to define an effective cross-section of capture of the droplets in cases when the plate is overheated (and W_c exceeds zero). The cross-section is fully determined by dimensionlessed radius η_e of an entrance region in plane $\xi = \xi^*$, such that all the droplets entering zone IV through this region impinge upon the plate and evaporate without recoil. Of course, η_e may be regarded as a single-valued function of η_{oe}. As w_c tends to zero, both these quantities go to infinity.

The curves of $f_o(\eta_o)$ within region $0 \leqslant \eta_o < \eta_e$ of the plate describe local flux of the dispersed liquid that in due course will vaporize. Thus they also determine the distribution over the plate of the local heat take-off caused by evaporation. On the contrary, all droplets that approach the plate outside the indicated region have to be almost elastically thrown away, in compliance with the physical model of refs. [9, 10]. They do not contribute to the heat removal, apart from a slight heat absorption that results from their quite negligible evaporation when remaining in the close vicinity of the plate for rather a short time. The last contribution may fairly be ignored.

Of great practical significance prove to be an effect of variation of distance h between the plate and jet nozzle under otherwise identical conditions. While the effect has usually remained beyond the framework of most experimental studies, there are good reasons to believe it to be capable of affecting to quite a considerable extent both total amount and local flux distribution of the captured droplets. Thus it must cause an appreciable influence on heat removal [16]. To address the problem, it is convenient to use curves of the same type as those in Fig. 5 but plotted in other dimensionless coordinates. Equation (2) clearly suggests d and U_d to be used as possible new length and velocity scales. Droplet flow rate distribution f_o^+ ($f_o^+(\eta_o^+)\,d\eta_o^+ = f_o(\eta_o)\,d\eta_o$) and dimensionless approach velocity $w^+ = W_n/U_d$ are shown as functions of $\eta_o^+ = r_o/d$ in Fig. 6 at $Stk = 10$ and different h/d. These curves are not so universal as those in Fig. 5 because their form depends on Stk. They have, how-

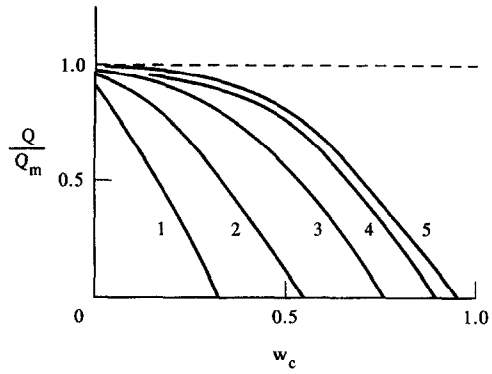

Fig. 7. Relative overall heat removal as a function of critical impact velocity; notation is the same as in Fig. 3.

ever, the advantage that dependence of relevant quantities on h/d becomes explicit. All other things being equal, the droplet flow rate distribution near the plate turns to be the more uniform, the farther the nozzle is situated. The evaporation region radius is to be determined with the help of the curves of Fig. 6, in just the same manner as when using Fig. 5.

4. HEAT ABSORPTION DUE TO VAPORIZATION

As it has already been pointed out, the droplet flow rate density at the plate completely determines the local heat take-off q per unit time caused by evaporation of liquid on the plate. If f_o is henceforth normalized to unity, we get

$$q = (4\pi/3)a^3\rho L f_o J = f_o Q_{max} \tag{7}$$

where L is the specific latent heat of evaporation and J stands for the number of droplets that pass through the nozzle for a unit time. The maximal heat Q_{max} corresponds then to complete evaporation of all the droplets. The overall heat removed from the plate during a unit time as a consequence of droplet vaporization is to be obtained by integrating expression (7) over the entire evaporation region. This yields

$$Q = 2\pi \int_0^{r_{oe}} q(r) r \, dr$$

$$= \left\{ 2\pi (r^*_{0.5})^2 \int_0^{\eta_{oe}} f_o(\eta_o)\eta_o \, d\eta_o \right\} Q_{max}. \tag{8}$$

If all the droplets were captured, η_{oe} would come to infinity, and the factor at Q_{max} in equation (8) would tend to unity.

As it has already been pointed out, dependence of q on diverse variables and parameters is exactly the same as that of f_o. Parametric dependence of Q is to be obtained by performing the integration of equation (8) with the help of the curves in either Fig. 5 or Fig. 6. By way of example, heat removal Q scaled with Q_{max} is presented in Fig. 7 as a function of dimensionless critical velocity w_c at different *Stk*. Ratio Q/Q_{max} tends to unity as w_c comes to zero. This simply means that there are no rejected droplets in the last case, and all of them ultimately vaporize on the plate. When w_c becomes sufficiently large, all the droplets rebound from the plate, and the heat removal due to evaporation disappears. Such a threshold value of w_c evidently decreases with the droplet size.

A deviation of the maximal value of Q/Q_{max} in Fig. 7 from unity for very small droplets presents an artefact. It has to be explained by the fact that the actual flow rate distribution of small droplets coming to the plate is rather flat in such cases, so that a significant number of droplets happens to fall outside the accepted region of numerical integration. Of course, those droplets are not taken into account while carrying out the calculation. To make the results more precise, the integration region must be somewhat broadened. It is worth noting that the aforementioned deviation can be used as an implicit indication on whether the numerical calculation may be regarded as an accurate one.

A relevant feature of curves in Fig. 7 consists in that the heat removal caused by evaporation declines as the critical impact velocity grows. The latter is a monotonously increasing function of the plate temperature [9], so that the curves may be viewed as representatives of the declining part of usually observed correlations between the whole heat removed for a unit time from a cooled surface and the surface temperature T_w in a so-called 'transient' temperature range. Many declining correlations of such a kind are reported in refs. [16–19] and in a great deal of other papers (see also Fig. 11 below).

An explicit equation relating Q/Q_{max} and T_w can be obtained by expressing w_c as a function of T_w in conformity with a formula in ref. [9],

$$T_w - T_s = W_c^2/\alpha \quad \alpha = 3\nu\lambda a/2\rho L\Delta^3 \tag{9}$$

where T_s is the saturation temperature, ν and λ are the vapor kinematic viscosity and thermal conductivity, respectively, and Δ is a characteristic length scale of the plate surface roughness. Since w_c is the dimensionless critical impact velocity W_c scaled with U^*, we next derive

$$w_c = [3\nu\lambda a(T_w - T_s)/2\rho\Delta^3 L(U^*)^2]^{1/2}. \tag{10}$$

This allows for recalculating Q/Q_{max} as a function of $T_w - T_s$ and comparing the result with experimental observations. A general character of this new dependence is the same as that of the curves in Fig. 7.

While leaving a detailed discussion until later, we wish to point out right away that the aforementioned dependence can be used to understand the occurrence of the declining section of experimental $Q - T_w$ curves. The contribution to heat transfer due to droplet evaporation usually plays a dominant role in the transient temperature range, so that this dependence may be viewed as one representative of the overall heat removal. Then the observed decrease of Q

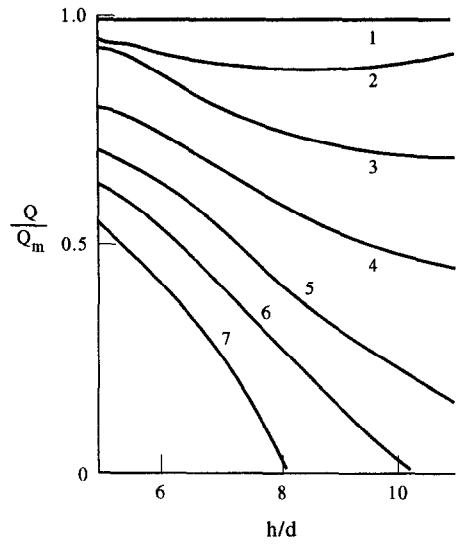

Fig. 8. Dependence of relative overall heat removal on dimensionless nozzle separation distance at $Stk = 10$ and $w_c^+ = 0.2$, 0.3, 0.4, 0.5, 0.6, 0.65 and 0.7 (curves 1–7, respectively).

accompanying an increase in T_w can successfully be explained by a corresponding reduction in the total amount of the dispersed liquid vaporized on a superheated surface.

A comparison of the theoretical inferences concerning the local heat take-off with experiments is somewhat hampered by the fact that most experimentalists commonly relate the total measured heat removal to some preassigned area. Consequently, they do not pay due attention to the fact that the effective area of droplet evaporation essentially diminishes and virtually vanishes as the surface temperature grows. This is why a precise quantitative correlation of most experimental data pertaining to the local heat transfer coefficient, with the above theoretical conclusions, seems often to be out of the question.

Next we turn to dependence of q and Q on dimensionless separation distance h/d. Since the distribution of q over the plate must be of the same form as that of f_0, it is in fact described by the curves of Fig. 6, and there is no need to dwell upon the question in more detail. Curves of Q/Q_{max} against h/d at different w_c^+ are drawn in Fig. 8. They evidence the overall heat removal to readily decrease as the nozzle is moved away from the plate, if the critical value of the droplet impact velocity is large enough. This is quite understandable because it is merely the droplets falling onto a central patch of the plate, just opposite the nozzle, that have a chance to overcome the excessive vapor pressure beneath the droplets [9, 10]. As the nozzle and the plate move apart, the patch rapidly diminishes and, further, disappears when the droplet approach velocity at its center falls below W_c. It is obvious that all the droplets must bounce off the plate if w_c^+ exceeds unity, no matter how small distance h.

The very character of the dependence of Q on h drastically changes, however, at comparatively low values of w_c^+. The heat removal becomes almost insensitive to variations of h in rather a broad interval. Moreover, it nearly coincides with its maximal value Q_{max} even if w_c^+ remains as high as 0.2. In the circumstance, it is apparently of no use to vary h in order to enhance Q. This notwithstanding, the alteration of the former variable at the latter one being practically constant, helps to extend the evaporation region. It might be useful to avoid the occurrence of dry spots and so to ensure relative uniformity of the local heat transfer coefficient. The pertinent dependence on h/d of the evaporation region radius scaled with d, η_{e0}^+, that can be inferred from Fig. 6 is illustrated in Fig. 9. The last quantity decreases when w_c^+ is high, but proves to be a monotonously increasing function of h/d in a range of smaller w_c^+.

The above inferences concerning q and Q as functions of diverse variables and parameters can seemingly provide for a useful tool, while designing spray cooling processes and improving their performance characteristics. To present a simple example, let us suppose, for the sake of definiteness, that we have in our disposal a device of parallel identical nozzles with fixed geometrical parameters to cool a surface of some given temperature above T_s. It seems to be a good policy to enlarge U_d in the first place so as to make w_c^+ lower than 0.2–0.3 (see Fig. 8). After that, it is reasonable to try to choose h/d in such a way as to gain a wanted degree of uniformity of the heat transfer over the surface, the droplet Stokes number being presumably known. Even so, there remains an additional parameter—the liquid concentration (or flow rate) at the nozzles—that may be adjusted to ensure a desired heat removal efficiency, not to mention that there is additional 'degree of freedom' stipulated by an opportunity to vary the droplet size and, consequently, the Stokes number. It must be emphasized once more that such a reasoning is only applicable under the condition of flow diluteness, when there are no thin liquid films on the cooled surface.

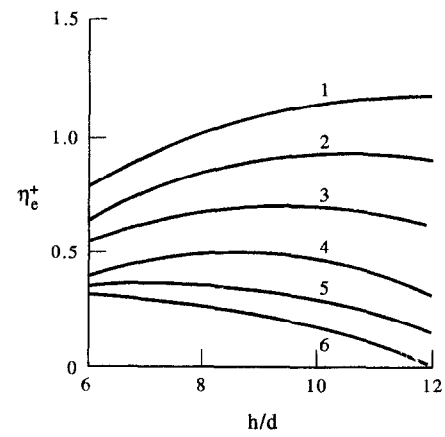

Fig. 9. Dimensionless radius η_{e0}^+ of evaporation region as a function of h/d at $Stk = 10$ and different w_c^+; notation is the same as in Fig. 8.

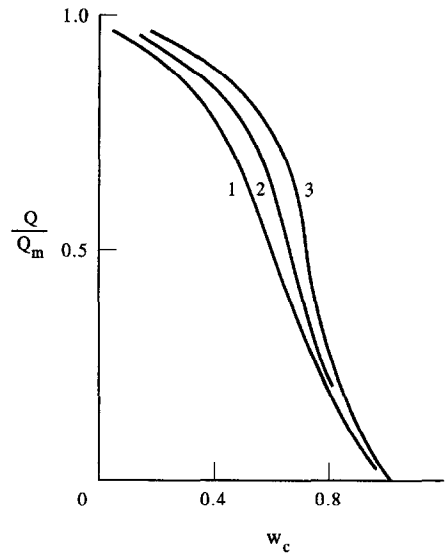

Fig. 10. Relative overall heat removal by polydisperse water spray as a function of w_c^+ for droplets of mean diameter $\langle 2a \rangle = 6 \times 10^{-5}$ m at different dispersion coefficients; 1–3—$\beta = 2$, 1.5 and 1.

5. POLYDISPERSE JETS

Practical realization of monodisperse spray flow is apparently a rather difficult engineering task, since it presents severe demands to the quality of devices used to pulverize the liquid. Commonly employed pulverizers are characterized by a more or less broad distribution of the droplets over size. The distribution may usually be described with the help of the log-normal law [15]

$$n(a) = (2\pi\sigma^2 a^2)^{-1/2} \exp\{-(1/2\sigma^2)[\lg(a/\langle a \rangle)]^2\}$$

$$\sigma^2 = \lg^2 \beta = \langle (\lg a - \lg \langle a \rangle)^2 \rangle \qquad (11)$$

with typical values of β ranging from 1.5 to 2.

Generalization of the model to such situations is trivial. Because of the supposed diluteness of two-phase flow, droplets of each size behave independently of droplets of all the other sizes. One can readily get a flow rate distribution at the plate for droplets of every size, by means of the developed calculation procedure. After that, the results have to be summed up or integrated with the statistical weight dictated by equation (11).

A specific feature of polydisperse mist flows as against monodisperse ones lies in that the boundary of the evaporation region on the plate, as well as on any other cooled surface, ceases to be sharp. It results from the fact that the boundary for identical droplets is dependent on their size. Thus, a transient region makes its appearance, in which larger droplets come to touching contact with the plate and vaporize whereas smaller droplets rebound and so do not take noticeable part in heat transfer.

To get a rough idea as to how the polydispersivity affects the performance of spray cooling devices, in Fig. 10 are drawn curves of Q/Q_{max} vs w_c at different dispersions of the droplet size distribution. Quantity Q can be seen to decrease as β grows, mean droplet radius $\langle a \rangle$ being fixed. It is also worth noting that the curves $Q - w_c$ become more gently sloping when β increases. The last effect is especially pronounced for relatively fine droplets, with Stk of the order of unity or smaller. At larger Stk, it turns out to be rather insignificant. Moreover, one may arrive at a conclusion about a certain insensitivity of the mentioned curves to changes in not only β but also Stk at $Stk \geqslant 10$ (cf. Fig. 6). This enables one to infer that there exists something like an asymptotic dependence of Q on w_c that holds approximately true in broad ranges of the aforementioned parameters, provided that the droplets are large enough. The conclusion proves to be useful to deduce, in a simple way, reliable theoretical predictions about the efficiency of spray cooling when the droplets are sufficiently large, as is frequently the case in engineering practice. It can also simplify to an extent correlation of experimental data as well as adaptation and refinement of the model.

6. DISCUSSION

The main issue of the presented treatment consists in that we have succeeded in exemplifying a general model of refs. [9, 10] by applying it to an important particular problem of spray cooling, also in bringing forward a calculation procedure needed to reveal dependence of heat transfer characteristics on key operating parameters. Even a superficial comparison of the model expectations with observations proves the former to be quite compatible with the whole bulk of experimental and industrial evidence as far as qualitative agreement is concerned.

There is a little doubt, if any, that it is the heat absorption caused by droplet evaporation that plays a dominant role in the transient temperature range in which the heat removal decreases monotonously as the cooled surface temperature grows. Therefore, the results obtained explain the very occurrence of such a range having been repeatedly observed in most experiments, and lend an additional support to the underlying physics discussed in refs. [9, 10]. What now remains to be done to be convinced of the adequacy of the model is to examine whether there is a satisfactory quantitative agreement between predictions on a basis of the developed theoretical scheme and available experimental data.

In spite of a great deal of experimental and industrial information on spray jet cooling, the last task is actually much more troublesome that it might seem from first glance. While measuring the overall heat removal per unit time Q or its density q as functions of the overheat $T_w - T_s$, experimentalists most commonly do not report on other pertinent parameters that are necessary, both to draw general conclusions of physical nature and to provide for a conclusive check of any model. If one puts in a summary chart of experimental curves of Q vs $T_w - T_s$ obtained by different

researchers, the curves will cover almost all the relevant area of the chart, in seemingly a casual and haphazard manner, sometimes with no discernible regularity. Examples of such summary diagrams are to be found in a number of publications and, in particular, on Fig. 1 of ref. [18] where 18 curves bearing upon water spray cooling are presented. Maximal values of the heat flux density at the beginning of the transient temperature range may differ under comparable conditions by more than an order of magnitude. At the same time, the scatter of observed values of the critical temperature at which the range starts comes up to a 100°C, or even more. A striking peculiarity lies in that the same is sometimes true even as far as experiments conducted under apparently identical conditions are concerned.

Reasons of such irreproducibility from experiment to experiment appear to be manifold. The most obvious one consists in that certain relevant parameters are repeatedly not controlled. For instance, the behavior of droplets approaching a superheated surface and, consequently, the onset of the heat transfer crisis depend, in compliance with the developed model, on the critical droplet impact velocity but not on the surface temperature alone. The last two variables are related between themselves by equation (9) which contains other parameters as well. In particular, coefficient α depends on the third power of the characteristic height Δ of surface rugosity, which itself is usually poorly determinable. Since this quantity varies in rather a wide range from 10^{-7} to 10^{-6} m even for high polished surfaces, an error in α may well amount up to three orders of magnitude. This is certainly more than sufficient to understand the scatter along the temperature axis.

Likewise, experimentalists frequently judge about the local heat flux density by relating the measured overall heat removal to a prescribed area that admittedly takes an active part in heat exchange. As it follows from the developed model and has already been indicated, those results can hardly be regarded as reliable, since the effective evaporation region is dependent on heat transfer conditions, especially so within the transient temperature range. (Some experiments in which the heat flux from a relatively small fixed test area is measured present an exception.) It can easily induce severe errors while determining the heat flux density, and thus may be responsible for the scatter along the other axis of q–$(T_w - T_s)$ diagrams. It has to be added that frequently air and water flow or velocities at the nozzle are merely reported. Such an important variable as the distance between the nozzle and cooled surface, that is capable of affecting the slope of these diagrams to a considerable degree, more often that not is left out of account.

It is reasonable in such a contingency to have recourse to only those experimental data that were obtained with the help of special heat exchange probes mounted into a cooled surface, under a condition that droplet evaporation positively occurred over the whole probe test area. Such a condition has been effected in the experiments of ref. [17] in which heat removal from a special disc probe was investigated. The disc was built into a horizontal plane, concentric to a water spray jet falling downward onto the plate surface from a nozzle situated at a distance of 10^{-1} m above the plate. The nozzle and the disc diameters were equal to 1.4×10^{-2} and 1.5×10^{-2} m, respectively. The jet velocity at the nozzle edge was of the order of 1 m s^{-1} or slightly less. The mean droplet diameter was high enough to ensure large values of the Stokes number. This allows one to safely ignore the droplet polydispersivity and to perform necessary calculations at $Stk = 10$, in conformity with the last remark of the preceding section.

In order to avoid the uncertainty associated with surface roughness, coefficient α involved in equation (9) was determined empirically, by making use of one of the experiments in ref. [17]. It is not difficult to show when using the curves of Fig. 6 that dimensionless critical impact velocity w_c^+ at the disc rim ($r/d \approx 0.5$) is approximately equal to 0.5, if $h/d \approx 7$ and $Stk = 10$. This means that $W_c \approx 0.2$ m s^{-1} for an experiment with $U_d = 0.432$ m s^{-1}. The critical temperature corresponding to the beginning of the transient temperature range in this experiment was $T_w = T_s + 46°C = 146°C$ [17]. Hence $\alpha \approx 10$, which enables us to draw theoretical q–$(T_w - T_s)$ curves within the whole transient range for all the experiments in the cited paper. In particular, we deduce that the critical temperature is 153 and 218°C for experiments with $U_d = 0.462$ and 0.724 m s^{-1}, respectively.

The theoretical and experimental curves are plotted in Fig. 11 whence it follows that correspondence between the model predictions and the experimental data is satisfactory. At the same time, the model somewhat overestimates both heat removal density and critical temperature at the largest jet velocity. This discrepancy may possibly be attributed to the jet becoming turbulent at high exit velocities, in consequence of which the droplets ought to disperse more intensively than they do under laminar flow conditions. Then the actual number of droplets hitting the test area is smaller than should be expected for a corresponding laminar jet. Naturally, this effect leads to cutting down the total amount of liquid to be vaporized and, consequently, to lessening heat removal as compared with the theoretical prediction. Furthermore, an increase in the jet exit velocity stipulates an increase in the droplet concentration in the vicinity of the plate, which brings about possible violation of the diluteness requirement inasmuch as the situation near the evaporation region is concerned. The total flux of the liquid to this region may also become too high to ensure the vapor outward flow being negligible, as it is required by the model. Then droplets coming to the plate experience an additional resistance that slows them down and, on the whole, reduces the surface temperature needed to throw them away. The dis-

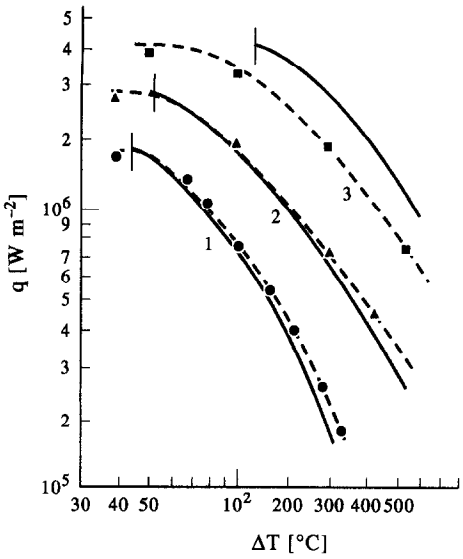

Fig. 11. Comparison of experimental data of ref. [17] (dots and dashed curves) with theoretical results for local heat removal density as a function of plate overheat, $T_w - T_s$ (solid curves); vertical lines mark the critical temperature resulting from the theory; 1–3 correspond to jet exit velocity U_d of 0.432, 0.462 and 0.724 m s^{-1}, respectively.

crepancy between the theoretical and experimental values of the critical temperature for the third experiment illustrated in Fig. 11 is perhaps due to just this reason.

It should be emphasized in conclusion that the model presented here and in refs. [9, 10] may also be useful in the matter of indicating those parameters that ought to be controlled in experiments in order to make them more informative and to avoid the irreproducibility. As regards the subsequent development of the model, possible directions of future work have been discussed in refs. [9, 10], and there is no need to repeat them again.

REFERENCES

1. R. Z. Alimov, Heat transfer in two-phase flow across a heated cylindrical tube, *Zh. Tekhn. Fiz.* **26,** 1292–1305 (1956) (in Russian).
2. H. Junk, Warmeubertragungs Untersuchungen an einer simulierten Secundarkuhlstrecke fur das Strangiesen von Stahl, *Neue Hutte H.* **1,** 13–18 (1972).
3. G. J. Hoogendorn and R. den Hond, Leidenfrost temperature and heat transfer coefficients for water sprays impinging on a hot surface, *Proceedings of the 5th Heat Transfer Conference*, Vol. 4, pp. 135–138, Tokyo (1974).
4. P. G. Kosky, Heat transfer to saturated mist flowing normally to a heated cylinder, *Int. J. Heat Mass Transfer* **19,** 539–543 (1976).
5. E. N. Ganic and W. M. Rohsenow, Dispersed flow heat transfer, *Int. J. Heat Mass Transfer* **20,** 855–866 (1977).
6. W. M. Rohsenow, Needed research in boiling heat transfer, In *Heat Transfer in Energy Problems*, pp. 51–58. Hemisphere, Washington (1983).
7. K. J. Choi and S. C. Yao, Mechanisms of film boiling heat transfer of normally impacting spray, *Int. J. Heat Transfer* **30,** 311–318 (1987).
8. S. Deb and S. G. Yao, Analysis of film boiling heat transfer of impacting sprays, *Int. J. Heat Mass Transfer* **32,** 2099–2112 (1989).
9. Yu. A. Buyevich and V. N. Mankevich, Interaction of dilute mist flow with a hot body, *Int. J. Heat Mass Transfer* **38,** 731–744 (1995).
10. K. N. Agafonov, Yu. A. Buyevich and V. N. Mankevich, To the theory of cooling of surfaces with drop-wise aerosol flow, *Teplofiz Vysokikh Temper.* **29,** 115–120 (1991) (in Russian).
11. G. N. Abramovich (ed.), *Theory of Turbulens Jets*. Nauka, Moscow (1984) (in Russian).
12. E. P. Dyban and A. I. Mazur, *Convective Heat Transfer in Jet Flows Around Bodies*. Naukova Dumka, Kiev (1982) (in Russian).
13. A. Rubbel, Numerical method to calculate flow of a jet onto a flat plate, *Raketnaya Tekhn. Cosmonavtika* **18,** 50–60 (1980) (in Russian).
14. K. N. Agafonov, A. D. Aralov and B. N. Yudaev, Study of the pressure distribution over a plate in axisymmetric jet flow, *Izvestiya VUZ-ov, Mashinostroyenie* **29,** 59–61 (1984) (in Russian).
15. N. A. Fuchs, *Mechanics of Aerosols*. Pergamon Press, New York (1964).
16. F. A. Mizikar, Spray cooling investigation for continuous casting of billestand blooms, *Iron Steel Engng* **47,** 53–60 (1970).
17. S. Toda, A study of mist cooling (1st report), *Heat Transfer—Jap. Res.* **1,** 39–50 (1972).
18. L. Bolle and J. Cl. Moureau, Spray cooling of hot surfaces: a description of the dispersed phase and a parametric study of heat transfer results, In *Two-Phase Flow and Heat Transfer*. Vol. III. *Proceedings of NATO Advanced Study Institute*, pp. 1327–1346 (1976).
19. E. I. Kazantsev *et al.*, Heat transfer in air-water cooling of a hot sheet, *Stahl*, **4,** 88–90 (1981) (in Russian).